

Differential Flatness as a Sufficient Condition to Generate Optimal Trajectories in Real Time

Logan E. Beaver, *Student Member, IEEE*, Michael Dorothy,
Christopher Kroninger, Andreas A. Malikopoulos, *Senior Member, IEEE*

Abstract—As robotic systems increase in autonomy, there is a strong need to plan efficient trajectories in real-time. In this paper, we propose an approach to significantly reduce the complexity of solving optimal control problems both numerically and analytically. We exploit the property of differential flatness to show that it is always possible to decouple the forward dynamics of the system’s state from the backward dynamics that emerge from the Euler-Lagrange equations. This coupling generally leads to instabilities in numerical approaches; thus, we expect our method to make traditional “shooting” methods a viable choice for optimal trajectory planning in differentially flat systems. To provide intuition for our approach, we also present an illustrative example of generating minimum-thrust trajectories for a quadrotor. Furthermore, we employ quaternions to track the quadrotor’s orientation, which, unlike the Euler-angle representation, do not introduce additional singularities into the model.

I. INTRODUCTION

Robotic systems continue to push the boundaries of autonomy in experimental testbeds [1]–[3] and outdoor experiments [4], [5]. As robotic systems achieve higher autonomy levels, they will be forced into complicated interactions with other agents [6] and the surrounding environment [7]. These autonomous robotic agents must be able to react quickly to their environment and re-plan efficient trajectories. To this end, we propose a new method to simplify real-time optimal trajectory planning by exploiting differential flatness.

While significant literature exists to solve optimal control problems for differentially flat systems, a majority of approaches transform the system into the flat output space and apply a fixed basis function to generate trajectories, e.g., polynomials [8], [9], Bezier curves [10], and Fourier decomposition [11]. Other approaches determine optimal waypoints at discrete instants in time and smoothly move between them [12]. In contrast, we exploit differential flatness to simplify the optimality conditions and solve for the optimal form of the trajectory.

Our main contribution is applying differential flatness to simplify the optimality conditions for continuous-time optimal control problems. These problems are, in general, two-point boundary problems for a set of nonlinear ordinary differential equations. The straightforward numerical

approach is to employ a *shooting method*, that is, to guess the missing boundary conditions at the initial time, integrate the differential equation forward to the final time, then use the error between the desired and actual final states to inform the next guess of the unknown initial state. This process is repeated until the numerical solution converges to the known boundary conditions. Unfortunately, the Euler-Lagrange equations that describe the evolution of the optimal state trajectory couple the system’s dynamics to a set of covector dynamics, and this leads to significant numerical instabilities [13], [14]. To resolve these instabilities, the standard approach is to select a nominal control input and integrate the system dynamics forward to the final state. Then, the Euler-Lagrange equations are integrated backward along the nominal trajectory. Finally, gradient descent is used at the initial and final boundaries to perturb the nominal control input and adjust the boundary conditions [13], [15]. In addition, a class of specialized solvers has emerged over the years to work around the instabilities inherent in the Euler-Lagrange equations [10], [11], [16].

Our main result proves that for any differentially flat system, the Euler-Lagrange equations can always be decoupled into two independent ordinary differential equations. The first describes the evolution of the state dynamics, and the second describes the evolution of the costate dynamics. Thus, we can solve for the evolution of the state and costate variables independently. Furthermore, we formulate a set of assumptions that allow us to discard the costate dynamics, and we present several approaches to relax these assumptions. Even after relaxing the assumptions, the states and costates are only coupled at the boundaries, and the evolution of the costates may be unnecessary to generate optimal state trajectories.

In addition to theoretical results, we present an illustrative example of a quadrotor operating in \mathbb{R}^3 . Many authors have taken differential flatness approaches to quadrotor dynamics [8], [9], [11], [17], [18]. However, all of these approaches represent the orientation of the quadrotor with Euler angles; this representation introduces additional singularities to the system, i.e., the gimbal lock phenomenon [9]. Instead, similar to [19], we employ quaternions to track the quadrotor’s orientation. Unlike [19], we derive the functions that transform the quadrotor state and control to the differentially flat outputs and derive the analytical closed-form solution for minimum-thrust trajectory generation.

The remainder of the manuscript is organized as follows. In Section II, we enumerate our assumptions and present our

This research was supported by the Delaware Energy Institute.

L.E. Beaver and A.A. Malikopoulos are with the Department of Mechanical Engineering, University of Delaware, Newark, DE (emails: lebeaver@udel.edu, andreas@udel.edu).

M. Dorothy and C. Kroninger are with Combat Capabilities Development Command, Army Research Laboratory, MD, USA. (emails: michael.r.dorothy.civ@mail.mil, christopher.m.kroninger.civ@mail.mil).

main theoretical result. We provide an illustrative example of our approach using a quadrotor in Section III. We present the closed-form differential flatness transform in Section III-C, and generate the minimum-thrust trajectory in Section III-D. We discuss relaxations of our assumptions in Section IV, and finally, we draw concluding remarks and present directions of future work in Section V.

II. MAIN RESULT

A. Differential Flatness Preliminaries

Consider the nonlinear dynamical system,

$$\dot{\mathbf{x}}(t) = \mathbf{f}(\mathbf{x}(t), \mathbf{u}(t)), \quad (1)$$

where $\mathbf{x}(t) \in \mathbb{R}^m$ and $\mathbf{u}(t) \in \mathbb{R}^n$ are the state and control vectors, respectively, and $t \in \mathbb{R}_+$ is time. A system is *differentially flat* if it satisfies the following definition [20].

Definition 1. A dynamical system with the form of (1) is differentially flat if and only if there exists a set of *flat outputs* $\mathbf{y}(t) \in \mathbb{R}^n$ and the functions

$$\mathbf{y}(t) = \boldsymbol{\sigma}(\mathbf{x}(t), \mathbf{u}(t), \dot{\mathbf{u}}(t), \dots, \mathbf{u}^{(p)}(t)), \quad (2)$$

$$\mathbf{x}(t) = \mathbf{g}(\mathbf{y}(t), \dot{\mathbf{y}}(t), \dots, \mathbf{y}^{(q)}(t)), \quad (3)$$

$$\mathbf{u}(t) = \mathbf{h}(\mathbf{y}(t), \dot{\mathbf{y}}(t), \dots, \mathbf{y}^{(r)}(t)), \quad (4)$$

where $p, q, r \in \mathbb{N}$, i.e., there exist mappings $\boldsymbol{\sigma}$, \mathbf{g} , and \mathbf{h} between the state and control variables and the flat outputs.

The outputs $\mathbf{y}(t)$ are also called *fictitious outputs*, as they do not necessarily have a physical interpretation. Importantly, Definition 1 enables us to transform a system with nonlinear dynamics into a space where the system obeys integrator dynamics. After generating the optimal trajectory in terms of the flat outputs, we apply Definition 1 to map the trajectory back to the initial space. Thus, we are able to generate the optimal trajectory without explicitly considering the constraints imposed by the nonlinear dynamics of the system.

B. Main Result

Consider the differentially flat system (Definition 1) with dynamics given by (1). We impose the following assumptions on the system.

Assumption 1. For the time interval $[t^0, t^f] \in \mathbb{R}$, the initial and final time, t^0 and t^f , are known and fixed a priori.

Assumption 2. The initial and final states, $\mathbf{x}(t^0)$ and $\mathbf{x}(t^f)$, are known and fixed a priori.

We only impose Assumptions 1 and 2 for completeness. These assumptions guarantee that our resulting boundary value problem has initial and final states that depend only on state and control variables. We discuss relaxations of these assumptions in Section IV.

Assumption 3. The transformation functions (2) - (4) exist everywhere.

We use Assumption 3 to guarantee that our differentially flat outputs always yield a corresponding state and control

trajectory for the system. Assumption 3 may be strong, as differential flatness is a property of the system dynamics. In reality, Definition 1 must only hold near the optimal trajectory, and it is possible to plan trajectories in the presence of certain singularities [17]. We discuss a relaxation of this assumption, motivated by our quadrotor example, in Section IV.

C. Flat Optimization Problem

Consider the general unconstrained optimal control problem under Assumptions 1 and 2.

Problem 1. Consider the differentially flat system with running cost $L(\mathbf{x}(t), \mathbf{u}(t))$ over the time horizon $[t^0, t^f] \subset \mathbb{R}$ and a final cost $\phi(\mathbf{x}(t^f), \mathbf{u}(t^f))$. Determine the optimal control input that minimizes the total cost,

$$\min_{\mathbf{u}(t)} \phi(\mathbf{x}(t^f), \mathbf{u}(t^f)) + \int_{t^0}^{t^f} L(\mathbf{x}(t), \mathbf{u}(t)) dt$$

subject to: (1),

$$\text{given: } \mathbf{x}(t^0), \mathbf{x}(t^f).$$

To solve Problem 1, we use the property of differential flatness (Definition 1). We denote the output vector $\mathbf{y}(t) = [y_1(t) \dots y_n(t)]^T$, and we may write the state and control of the system, $\mathbf{x}(t)$ and $\mathbf{u}(t)$, in terms of $\mathbf{y}(t)$ and a finite number of derivatives. All elements of $\mathbf{y}(t)$ may not require the same number of derivatives to satisfy Definition 1; thus, we denote the required number of derivatives as k_1, k_2, \dots, k_n for the n elements of $\mathbf{y}(t)$. This yields integrator dynamics,

$$y_i^{(j)}(t) = y_i^{(j+1)}(t), \quad (5)$$

for $i \in \{1, 2, \dots, n\}$ and $j \in \{0, 1, \dots, k_i - 1\}$. Next, we define equivalent state and control vectors for the flat output system.

Definition 2. The integrator dynamics of (5) describe an equivalent dynamical system in the output space, which consists of the state vector $\mathbf{s}(t)$ and control vector $\mathbf{a}(t)$,

$$\mathbf{s}(t) = [y_1(t), \dots, y_1^{(k_1-1)}(t), \dots, y_n(t), \dots, y_n^{(k_n-1)}(t)]^T, \quad (6)$$

$$\mathbf{a}(t) = [y_1^{(k_1)}(t), \dots, y_n^{(k_n)}(t)]^T. \quad (7)$$

We propose an equivalent optimal control problem in the flat output space defined by Definition 2.

Problem 2. Consider the system described by Definition 2. Given a running cost $\Psi(\mathbf{s}(t), \mathbf{a}(t))$ over the time horizon $[t^0, t^f] \subset \mathbb{R}$ and a final cost $\Phi(\mathbf{s}(t^f), \mathbf{a}(t^f))$, determine the optimal control action that minimizes the total cost,

$$\min_{\mathbf{a}(t)} \Phi(\mathbf{s}(t^f), \mathbf{a}(t^f)) + \int_{t^0}^{t^f} \Psi(\mathbf{s}(t), \mathbf{a}(t)) dt$$

subject to: (5),

$$y_i^{(j)}(t^0) = \frac{d^j}{dt^j} \left[\sigma_i(\mathbf{x}(t), \mathbf{u}(t), \dots, \mathbf{u}^{(q)}(t)) \right]_{t^0},$$

$$y_i^{(j)}(t^f) = \frac{d^j}{dt^j} \left[\sigma_i(\mathbf{x}(t), \mathbf{u}(t), \dots, \mathbf{u}^{(q)}(t)) \right]_{t^f},$$

where $i \in \{1, 2, \dots, n\}$, $j \in \{0, 1, 2, \dots, k_i\}$, and σ_i are the rows of σ in Definition 1.

Lemma 1. There exists an endpoint and running cost for Problem 2 such that it is equivalent to Problem 1.

Proof. Under Assumption 3, we compose the functions \mathbf{g} and \mathbf{h} (Definition 1) with L and ϕ , yielding

$$\Psi(\mathbf{s}(t), \mathbf{a}(t)) = L(\mathbf{g}(\mathbf{s}(t), \mathbf{a}(t)), \mathbf{h}(\mathbf{s}(t), \mathbf{a}(t))), \quad (8)$$

$$\Phi(\mathbf{s}(t^f), \mathbf{a}(t^f)) = \phi(\mathbf{g}(\mathbf{s}(t^f), \mathbf{a}(t^f)), \mathbf{h}(\mathbf{s}(t^f), \mathbf{a}(t^f))). \quad (9)$$

This implies that the costs of Problems 1 and 2 are equal. Thus, the optimal solution to Problem 2 minimizes the cost of Problem 1 while satisfying the boundary conditions and dynamics. \square

Note that although the boundary conditions of Problem 2 appear challenging, they do not present a problem for our approach. Next, we present a result, where we decouple the forward state dynamics from the backward costate dynamics for Problem 2.

Theorem 1. The optimal control input $\mathbf{a}^*(t)$ that minimizes Problem 2 can always be determined by an ordinary differential equation that is only a function of the state and control variables.

Proof. We follow the standard process for solving optimal control problems [15], [16]. First, we construct the Hamiltonian for Problem 2,

$$H = \Psi(\mathbf{s}(t), \mathbf{a}(t)) + \boldsymbol{\lambda}^T(t) \mathbf{I}(\mathbf{s}(t), \mathbf{a}(t)), \quad (10)$$

where $\boldsymbol{\lambda}(t)$ is the vector of costates and $\mathbf{I}(\mathbf{s}(t), \mathbf{a}(t))$ corresponds to the integrator dynamics defined by (5).

To simplify the notation, we omit the explicit dependence on $\mathbf{a}(t)$ and $\mathbf{s}(t)$ where it does not lead to ambiguity. The corresponding Euler-Lagrange equations are

$$\Psi_{\mathbf{a}} + \boldsymbol{\lambda}^T \mathbf{I}_{\mathbf{a}} = 0, \quad (11)$$

$$-\dot{\boldsymbol{\lambda}} = \Psi_{\mathbf{s}} + \boldsymbol{\lambda}^T \mathbf{I}_{\mathbf{s}}, \quad (12)$$

where the subscripts \mathbf{a} and \mathbf{s} correspond to formal partial derivatives with respect to the output action and state, respectively (Definition 2). We simplify (12) by exploiting the integrator structure of \mathbf{I} for each element of $\mathbf{s}(t)$, this yields

$$\dot{\lambda}^{y_i} = -\Psi_{y_i}, \quad (13)$$

$$\dot{\lambda}^{y_i^{(k)}} = -\Psi_{y_i^{(k)}} - \lambda^{y_i^{(k-1)}}, \quad (14)$$

for $i \in \{1, 2, \dots, n\}$ and $k \in \{1, 2, \dots, k_i - 1\}$. Similarly, simplifying (11) yields,

$$\lambda^{y_i^{(k_i-1)}} = -\Psi_{\alpha_i} \quad (15)$$

for each output $i \in \{1, 2, \dots, n\}$. Taking a time derivative of (15) and substituting it into (14) with $k = k_i - 1$ yields

$$\frac{d}{dt} \Psi_{\alpha_i} = \Psi_{y_i^{(k_i-1)}} + \lambda^{y_i^{(k_i-2)}}. \quad (16)$$

Note that (14) equates the time derivative of the k^{th} costate to the $k-1^{\text{th}}$ costate. Thus, by taking repeated time derivatives

of (16) and substituting (14) into the resulting equation at each step, we reach an ordinary differential equation composed of partial derivatives of Ψ and λ^{y_i} . Finally, substituting (13) yields

$$\sum_{j=0}^{k_i} (-1)^j \frac{d^j}{dt^j} \Psi_{y_i^{(j)}} = 0, \quad (17)$$

which holds for each flat output $y_i(t)$, $i = 1, 2, \dots, n$. Thus, (17) is an equivalent optimality condition for the optimal solution to Problem 2, and furthermore (17) is only a function of the state and control variables. \square

Note that the decoupled ordinary differential equation (17) does not need to be solved in the output space, and it can be transformed back to the original space of Problem 1.

Corollary 1. For a differentially flat system under Assumptions 1-3, the optimal control function that minimizes Problem 1 can always be determined independently of the costate equations.

Proof. Under Assumption 3, composing (17) with (2) yields an ordinary differential equation that describes the evolution of the state and control variables of Problem 1. By Assumptions 1 and 2, the boundary conditions of this differential equation are fixed. Thus, the optimal control input can be determined analytically or numerically by solving an ordinary differential equation with known boundary conditions without considering the costate dynamics. \square

In the following section, we present an illustrative example of the differentially flat quadrotor model. We augment the quadrotor dynamics with a quaternion to remove the singularities generally introduced by Euler angles [9] and fully derive the equivalent version of Problem 2 for minimum-thrust control.

III. QUADROTOR EXAMPLE

A. Quaternions Preliminaries

In Section III, we employ unit quaternions to track the orientation of the quadrotor in the global reference frame. Unit quaternions are an alternative to rotation matrices, and they are capable of tracking rotations in \mathbb{R}^3 using a single axis and rotation angle [21], [22]. We denote quaternions with a bold face and overbar, thus $\bar{\mathbf{q}}(t) \in \mathbb{R}^4$. Quaternions have a so-called *scalar* and *vector* part, which we define,

$$\bar{\mathbf{q}}(t) := \cos(\theta(t)) + \begin{bmatrix} u(t) \\ v(t) \\ w(t) \end{bmatrix} \sin(\theta(t)), \quad (18)$$

where $\cos(\theta(t))$ is the scalar part of the quaternion, the vector $[u(t), v(t), w(t)]^T \in \mathbb{R}^3$ denotes an axis, and $\theta(t) \in \mathbb{R}$ denotes a rotation about the axis. Finally, $\bar{\mathbf{q}}$ is a unit quaternion when $\sqrt{u^2 + v^2 + w^2} = 1$.

Quaternion multiplication is defined using the Hamilton product, and the product of two unit quaternions always yields a unit quaternion. To multiply a vector $\mathbf{r} \in \mathbb{R}^3$ with a quaternion $\bar{\mathbf{q}} \in \mathbb{R}^4$, we construct the quaternion $\bar{\mathbf{r}}$ with zero real part and a vector part equal to \mathbf{r} , i.e., via (18),

$\cos(\theta) = 0$, $\sin(\theta) = 1$, and $[u, v, w]^T = \mathbf{r}$. We take the product of $\bar{\mathbf{r}}$ and $\bar{\mathbf{q}}$, which always yields a quaternion with zero real part and a vector part equal to the new value of \mathbf{r} . See [21] for further discussion of Quaternions and their properties.

B. Dynamics

Consider a quadrotor whose center of mass is described by the vector $\mathbf{p}(t) \in \mathbb{R}^3$. Let $\mathbf{z}_g = [0, 0, 1]^T$ be the direction of gravity in the global reference frame and $\bar{\mathbf{q}}(t)$ be the unit quaternion that describes the orientation of the quadrotor relative to the fixed global reference frame. A schematic of the quadrotor and its relevant axes is shown in Fig. 1.

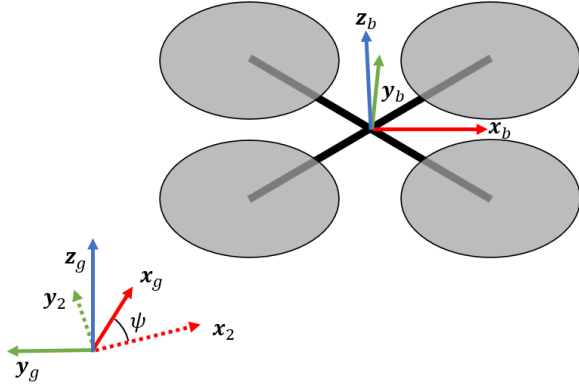


Fig. 1. Schematic of the quadrotor with the global (subscript g), local (subscript b), and intermediate (subscript 2) coordinate transformations annotated.

Applying Newton's second law to the center of mass of the the quadrotor yields the second order dynamics [9], [19],

$$\dot{\mathbf{p}}(t) = \mathbf{v}(t), \quad (19)$$

$$\dot{\mathbf{v}}(t) = -g\mathbf{z}_g + \frac{T(t)}{m}\bar{\mathbf{q}}(t)\mathbf{z}_g\bar{\mathbf{q}}^{-1}(t), \quad (20)$$

where g is acceleration due to gravity, $T(t)$ is the collective thrust imposed by the quadrotor's propellers, m is the quadrotor's mass, and $\bar{\mathbf{q}}(t)\mathbf{z}_g\bar{\mathbf{q}}^{-1}(t)$ is a unit vector colinear to the quadrotor's thrust vector (\mathbf{z}_b in Fig. 1). The rate of change of the quadrotor's orientation is given by the relation [22]

$$\dot{\bar{\mathbf{q}}}(t) = \frac{1}{2}\boldsymbol{\omega}(t)\bar{\mathbf{q}}(t), \quad (21)$$

where $\boldsymbol{\omega}(t) \in \mathbb{R}^3$ is the angular velocity of the quadrotor in the local coordinate frame. Finally, applying Newton's second law for rotation yields [9], [19],

$$\boldsymbol{\tau}(t) = J\dot{\boldsymbol{\omega}}(t) + \boldsymbol{\omega}(t) \times (J \cdot \boldsymbol{\omega}(t)), \quad (22)$$

where J is a constant inertial matrix and $\boldsymbol{\tau}(t)$ is the vector of torques applied about the local axes ($[\mathbf{x}_b, \mathbf{y}_b, \mathbf{z}_b]$ in Fig. 1). Rearranging (22) yields

$$\dot{\boldsymbol{\omega}}(t) = J^{-1}\left(\boldsymbol{\tau}(t) - \boldsymbol{\omega}(t) \times (J \cdot \boldsymbol{\omega}(t))\right). \quad (23)$$

Therefore, the quadrotor's state is the time-varying vector

$$\mathbf{x}(t) = \begin{bmatrix} \mathbf{p}(t) \\ \mathbf{v}(t) \\ \bar{\mathbf{q}}(t) \\ \boldsymbol{\omega}(t) \end{bmatrix} \in \mathbb{R}^{3 \times 3 \times 3 \times 3}, \quad (24)$$

with dynamics given by (19) - (21) and (23), and the control input

$$\mathbf{u}(t) = \begin{bmatrix} T(t) \\ \boldsymbol{\tau}(t) \end{bmatrix} \in \mathbb{R}^4. \quad (25)$$

C. Flatness Transform

An appropriate flat output vector $\mathbf{y}(t) \in \mathbb{R}^4$ is [8],

$$\mathbf{y}(t) = \begin{bmatrix} \mathbf{p}(t) \\ \psi(t) \end{bmatrix}, \quad (26)$$

where $\psi(t)$ is the yaw angle, i.e., the quadrotor's rotation relative to \mathbf{z}_g , which can be determined from $\bar{\mathbf{q}}(t)$. Additionally, the states $\mathbf{p}(t)$ and $\mathbf{v}(t)$ are trivially functions of $\mathbf{y}(t)$ and $\dot{\mathbf{y}}(t)$. Rearranging (20) yields

$$m(\dot{\mathbf{v}}(t) + g\mathbf{z}_g) = T(t)\bar{\mathbf{q}}(t)\mathbf{z}_g\bar{\mathbf{q}}^{-1}(t), \quad (27)$$

which has a magnitude of

$$|T(t)| = m\sqrt{\dot{x}(t)^2 + \dot{y}(t)^2 + (\dot{z}(t) + g)^2}, \quad (28)$$

aligned with $\bar{\mathbf{q}}(t)\mathbf{z}_g\bar{\mathbf{q}}(t)^T$. Thus, the thrust control satisfies Definition 1.

Next, we decompose $\bar{\mathbf{q}}$ into two rotations, one of angle ψ about \mathbf{z}_g and a second of angle $\theta \in \mathbb{R}$ about the unit vector $[u, v, 0]^T$, i.e.,

$$\bar{\mathbf{q}} = \bar{\mathbf{q}}_R \bar{\mathbf{q}}_\psi, \quad (29)$$

where

$$\bar{\mathbf{q}}_\psi(t) = \cos \frac{\psi}{2} + \mathbf{z}_g \sin \frac{\psi}{2}, \quad (30)$$

corresponds to the yaw of the quadrotor relative to the fixed coordinate frame, i.e., $[\mathbf{x}_2, \mathbf{y}_2, \mathbf{z}_g]$ in Fig. 1, and

$$\bar{\mathbf{q}}_R = \cos \frac{\theta}{2} + \begin{bmatrix} u \\ v \\ 0 \end{bmatrix} \sin \frac{\theta}{2}. \quad (31)$$

is a second rotation that brings the quadrotor to its final orientation, i.e., $[\mathbf{x}_b, \mathbf{y}_b, \mathbf{z}_b]$ in Fig. 1. Substituting (29) into (20) and rearranging yields

$$\dot{\mathbf{v}}(t) + g\mathbf{z}_g = \frac{T(t)}{m}\bar{\mathbf{q}}_R(\bar{\mathbf{q}}_\psi\mathbf{z}_g\bar{\mathbf{q}}_\psi^{-1})\bar{\mathbf{q}}_R^{-1}. \quad (32)$$

As $\bar{\mathbf{q}}_\psi$ corresponds to a rotation about the \mathbf{z}_g axis, $\bar{\mathbf{q}}_\psi\mathbf{z}_g\bar{\mathbf{q}}_\psi^{-1} = \mathbf{z}_g$. Thus,

$$\dot{\mathbf{v}}(t) + g\mathbf{z}_g = \frac{T(t)}{m}\bar{\mathbf{q}}_R\mathbf{z}_g\bar{\mathbf{q}}_R^{-1}. \quad (33)$$

Eq. (33) introduces a singularity when $\dot{\mathbf{v}}(t) + g\mathbf{z}_g = \mathbf{0}$, i.e., the quadrotor is in free fall and $\bar{\mathbf{q}}_R$ can be arbitrarily selected. Thus, to satisfy Assumption 3, we impose that $\dot{\mathbf{v}}(t) \neq -g\mathbf{z}_g$ for the remainder of our derivation.

Let

$$\hat{\mathbf{c}}(t) = \frac{\dot{\mathbf{v}}(t) + g\mathbf{z}_g}{\|\dot{\mathbf{v}}(t) + g\mathbf{z}_g\|} \quad (34)$$

be the unit vector that points in the direction of the quadrotor's thrust. Substituting $\hat{\mathbf{c}}(t)$ into (33), rearranging, and right multiplying by $\bar{\mathbf{q}}_R$ yields

$$\hat{\mathbf{c}}(t) \bar{\mathbf{q}}_R(t) = \bar{\mathbf{q}}_R(t) \mathbf{z}_g. \quad (35)$$

Quaternion multiplication is non-commutative, therefore (35) yields a system of equations to solve for the unknown angle θ and axis $[u, v, 0]^T$ that define (31). Let $[c_x(t), c_y(t), c_z(t)]^T$ be the components of $\hat{\mathbf{c}}(t)$; for notational simplicity we will omit the explicit dependence of variables on time where no ambiguity arises. Equating the scalar component of (35) yields

$$u = \pm \frac{c_y}{\sqrt{1 - c_z^2}}, \quad (36)$$

$$v = \mp \frac{c_x}{\sqrt{1 - c_z^2}}, \quad (37)$$

while each vector component of (35) yields the identical equation

$$\theta = 2 \arctan \left(\mp \frac{\sqrt{c_x^2 + c_y^2}}{1 + c_z} \right), \quad (38)$$

which is feasible when $c_z^2 \neq 1$. If $c_z^2 = 1$, then $c_x = c_y = 0$ and $\hat{\mathbf{c}}$ is parallel to \mathbf{z}_b . This implies, by (35), that $\theta = 0$ or $\theta = \pi$, and thus u, v may be arbitrarily selected.

Eqs. (36) - (38) each have two solutions. Both solutions yield a unit quaternion that rotates the quadrotor in opposite directions about opposite axes. We select the second solution of each equation, and thus $\bar{\mathbf{q}}(t)$ satisfies Definition 1.

Next, rearranging (21) yields

$$\boldsymbol{\omega}(t) = 2 \dot{\bar{\mathbf{q}}}(t) \bar{\mathbf{q}}(t)^{-1}, \quad (39)$$

thus $\boldsymbol{\omega}(t)$ satisfies Definition 1. We expand (39) and substitute (36) - (38), which yields

$$\boldsymbol{\omega}(t) = \begin{bmatrix} \dot{\psi} c_x - \dot{c}_y + \frac{c_y \dot{c}_z}{1 + c_z} \\ \dot{\psi} c_y + \dot{c}_x - \frac{c_x \dot{c}_z}{1 + c_z} \\ \dot{\psi} c_z + \frac{\dot{c}_x c_y - \dot{c}_y c_x}{1 + c_z} \end{bmatrix}. \quad (40)$$

Finally, $\boldsymbol{\tau}(t)$ is a function of $\boldsymbol{\omega}$ and $\dot{\boldsymbol{\omega}}(t)$ by (22). Thus, $\boldsymbol{\tau}(t)$ satisfies Definition 1. As $\mathbf{x}(t)$ and $\mathbf{u}(t)$ can both be written as an explicit function of the flat outputs, $\mathbf{y}(t)$, and a finite number of time derivatives, the quadrotor system is differentially flat.

The highest derivatives of our flat outputs that appear in the transformations are $\frac{d^4}{dt^4} \mathbf{p}$ and $\frac{d^2}{dt^2} \psi(t)$. Thus, following Definition 2, we group the output variables into the state and control vectors,

$$\mathbf{x}'(t) = [\mathbf{p}^T(t) \mathbf{v}^T(t) \mathbf{a}^T(t) \mathbf{j}^T(t) \psi(t) \omega_z(t)]^T, \quad (41)$$

$$\mathbf{u}'(t) = [\mathbf{s}^T(t) \alpha_z(t)]^T, \quad (42)$$

i.e., we will control the *snap* and *yaw acceleration* of the quadrotor subject to integrator dynamics on the position and yaw angle. Next, we present an illustrative example that applies Theorem 1 to the problem of generating the minimum-thrust trajectory.

D. Minimum-Thrust Trajectory

Consider the problem of moving a quadrotor between two fixed states while minimizing the L^2 norm of thrust, given by (28).

Problem 3. Let the vector $\mathbf{u}(t) = [\mathbf{s}^T, \alpha_z]^T$ be the snap and yaw acceleration of the quadrotor in the global reference frame. For a given horizon $[t^0, t^f] \subset \mathbb{R}$, and a particular initial and final state, generate the trajectory that minimizes the L^2 norm of the quadrotor's thrust,

$$\min_{\mathbf{s}(t), \alpha_z(t)} \frac{1}{m^2} \int_{t^0}^{t^f} \|\mathbf{a}(t) + g\mathbf{z}_g\|^2 dt$$

subject to:

$$\dot{\mathbf{x}}(t) = \mathbf{I}(\mathbf{x}(t), \mathbf{u}(t)),$$

given:

$$\mathbf{p}(t^0), \mathbf{v}(t^0), \hat{\mathbf{c}}(t^0), \dot{\hat{\mathbf{c}}}(t^0)$$

$$\mathbf{p}(t^f), \mathbf{v}(t^f), \hat{\mathbf{c}}(t^f), \dot{\hat{\mathbf{c}}}(t^f),$$

where $\mathbf{I}(\mathbf{x}(t), \mathbf{u}(t))$ is the integrator dynamics of the system defined by (41). Note that under Assumption 2 it is trivial to determine the boundary values for $\hat{\mathbf{c}}$ from (35). Likewise, (40) provides a system of linear equations that yields $\dot{\hat{\mathbf{c}}}$ at the boundaries.

Applying (17) to the rotational states and corresponding control $\alpha_z(t)$ implies that any functional form of $\alpha_z(t)$ that satisfies the initial and boundary conditions is optimal. This follows trivially from the fact that Problem 3's objective function does not contain rotational terms.

Applying (17) to the translational states and corresponding control $\mathbf{s}(t)$ yields

$$\frac{d^2}{dt} \left(\frac{\partial}{\partial \mathbf{a}} \left\{ (\mathbf{a}(t) + g\mathbf{z}) \cdot (\mathbf{a}(t) + g\mathbf{z}) \right\} \right) = \mathbf{0}, \quad (43)$$

which simplifies to

$$\mathbf{s}^*(t) = \mathbf{0}, \quad (44)$$

i.e., all zero snap trajectories minimize the L^2 norm of the quadrotor's thrust. Integrating (44) yields the optimal acceleration profile

$$\mathbf{a}^*(t) = \mathbf{c}_1 t + \mathbf{c}_2, \quad (45)$$

where \mathbf{c}_1 and \mathbf{c}_2 are constants of integration that are determined by boundary conditions on $\mathbf{p}(t)$ and $\mathbf{v}(t)$ in Problem 3. Motivated by the linear form of $\mathbf{a}^*(t)$, we present several approaches to extend our analysis and relax Assumptions 1-3 in the following section.

IV. EXTENSIONS

The form of (45) provides insight into how one might relax Assumption 3. Recall the singularity imposed by (33), and let $\mathbf{a}(t_1) = -g\mathbf{z}_g$ for some $t_1 \in [t^0, t^f]$. This leads to two possible cases.

Case I: $\mathbf{c}_1 = \mathbf{0}$. If $\mathbf{a}(t_1) = -g\mathbf{z}_b$, then $\mathbf{c}_2 = -g\mathbf{z}_b$. This implies that the quadrotor is in free-fall for all $t \in [t^0, t^f]$, and the optimal thrust is $T(t) = 0$ for all $t \in [t^0, t^f]$.

Case II: $\mathbf{c}_1 \neq \mathbf{0}$. If $\mathbf{a}(t_1) = -g\mathbf{z}_b$, then the singularity can only occur instantaneously at $t = t_1$. Thus, the optimal state $\mathbf{x}^*(t_1)$ can be determined by exploiting continuity in the state i.e., $\lim_{t \rightarrow t_1} \mathbf{x}^*(t) = \mathbf{x}^*(t_1)$.

Relaxing Assumption 2 implies that at least one initial or final state is left unspecified in Problem 1. Without loss of generality, let the state $p(t)$ be unspecified at t^0 . This implies that $p(t^0)$ can be arbitrarily selected. It follows that any output state $q(t)$ that is an explicit function of $p(t)$ is also arbitrary at t^0 , and thus $\lambda^q(t^0) = 0$ [15]. We substitute this condition into (13) - (15) to determine an additional initial condition for the states and control variables in Problem 2. Similarly, one could examine the Euler-Lagrange equations in the original space (Problem 1) to determine an additional boundary condition on the original state and control variables.

We may relax Assumption 1 by taking t^f to be an unknown optimization variable in Problems 1 and 2. The optimal terminal time must satisfy [15] $\left(\frac{\partial \Phi}{\partial t} + \lambda^T \mathbf{I} + \Psi\right)\Big|_{t^f} = 0$, which results in a set of equations for $\lambda(t^f)$, given the integrator dynamics. These equations can be combined with (13) - (15) to yield additional conditions for the optimal stopping time t^f .

Finally, it is possible to include constraints in Problems 1 and 2. Any constraint of the form $\mathbf{g}(\mathbf{x}(t), \mathbf{u}(t), t) \leq \mathbf{0}$ can be composed with (3) and (4) to yield an equivalent set of constraints on Problem 2. In general, to solve the constrained version of Problem 2 we generate a constrained motion primitive for each combination of constraints that may become active [23], [24]. This is analogous to relaxing Assumptions 1 and 2 simultaneously. It is particularly straightforward to include constraints that only depends on $\mathbf{y}(t)$ and its derivatives, as their transformation to the output space is trivial.

V. CONCLUSION

In this paper, we proposed a method that we expect to significantly reduce the computational requirements of generating optimal trajectories for systems with differentially flat dynamics. In particular, we presented a technique to decouple the state evolution equation from the dynamics of the costates. This result, in general, resolves a fundamental challenge associated with solving optimal control problems, both numerically and analytically [14]. Finally, we presented several feasible approaches to relax the assumptions that we impose for our solution.

There are several intriguing directions for future work. First, it is practical, for given dynamics, to determine what functional forms of the objective guarantee that an analytical solution to (17) exists. A potential direction for future research is to relax Assumption 3 and manage singularities in the flatness transformations. Finally, leveraging traditional shooting approaches to generate optimal trajectories in real time is another potential research direction.

REFERENCES

- [1] M. Rubenstein, C. Ahler, and R. Nagpal, "Kilobot: A low cost scalable robot system for collective behaviors," in *Proceedings of the 2012 IEEE International Conference on Robotics and Automation*, 2012.
- [2] K. Jang, E. Vinitsky, B. Chalaki, B. Remer, L. Beaver, A. A. Malikopoulos, and A. Bayen, "Simulation to scaled city: zero-shot policy transfer for traffic control via autonomous vehicles," in *Proceedings of the 10th ACM/IEEE International Conference on Cyber-Physical Systems*, 2019, pp. 291–300.
- [3] L. E. Beaver, B. Chalaki, A. M. Mahbub, L. Zhao, R. Zayas, and A. A. Malikopoulos, "Demonstration of a Time-Efficient Mobility System Using a Scaled Smart City," *Vehicle System Dynamics*, vol. 58, no. 5, pp. 787–804, 2020.
- [4] G. Vásárhelyi, C. Virágh, G. Somorjai, T. Nepusz, A. E. Eiben, and T. Vicsek, "Optimized flocking of autonomous drones in confined environments," *Science Robotics*, vol. 3, no. 20, 2018.
- [5] A. M. I. Mahbub and A. Malikopoulos, "Concurrent optimization of vehicle dynamics and powertrain operation using connectivity and automation," in *SAE Technical Paper 2020-01-0580*. SAE International, 2020.
- [6] L. E. Beaver and A. A. Malikopoulos, "An Overview on Optimal Flocking," *arxiv:2009.14279*, 2020.
- [7] H. Oh, A. R. Shirazi, C. Sun, and Y. Jin, "Bio-inspired self-organising multi-robot pattern formation: A review," *Robotics and Autonomous Systems*, vol. 91, pp. 83–100, 2017.
- [8] D. Mellinger and V. Kumar, "Minimum snap trajectory generation and control for quadrotors," in *IEEE International Conference on Robotics and Automation*, 2011, pp. 2520–2525.
- [9] K. Sreenath, N. Michael, and V. Kumar, "Trajectory generation and control of a quadrotor with a cable-suspended load - A differentially-flat hybrid system," in *IEEE International Conference on Robotics and Automation*, 2013, pp. 4888–4895.
- [10] M. B. Milam, "Real-Time Optimal Trajectory Generation for Constrained Dynamical Systems," Ph.D. dissertation, California Institute of Technology, 2003.
- [11] O. T. Ogunbodede, "Optimal Control of Differentially Flat Systems," Ph.D. dissertation, The University at Buffalo, 2020.
- [12] M. J. Van Nieuwstadt and R. M. Murray, "Real-Time Trajectory Generation for Differentially Flat Systems," *International Journal of Robust and Nonlinear Control*, vol. 8, pp. 995–1020, 1998.
- [13] A. E. Bryson and W. F. Denham, "A steepest-ascent method for solving optimum programming problems," *Journal of Applied Mechanics*, vol. 29, no. 2, pp. 247–257, 1962.
- [14] A. E. Bryson, "Optimal Control-1950 to 1985," *IEEE Control Systems Magazine*, vol. 16, no. 3, pp. 26–33, 1996.
- [15] A. E. J. Bryson and Y.-C. Ho, *Applied Optimal Control: Optimization, Estimation, and Control*. John Wiley and Sons, 1975.
- [16] I. M. Ross, *A Primer on Pontryagin's Principle in Optimal Control*, 2nd ed., E. Solon, Ed. San Francisco: Collegiate Publishers, 2015.
- [17] B. Morrell, M. Rigter, G. Merewether, R. Reid, R. Thakker, T. Tzanetos, V. Rajur, and G. Chamitoff, "Differential Flatness Transformations for Aggressive Quadrotor Flight," in *IEEE International Conference on Robotics and Automation*, 2018, pp. 5204–5210.
- [18] M. Faessler, A. Franchi, and D. Scaramuzza, "Differential Flatness of Quadrotor Dynamics Subject to Rotor Drag for Accurate Tracking of High-Speed Trajectories," *IEEE Robotics and Automation Letters*, vol. 3, no. 2, pp. 620–626, 4 2018.
- [19] E. Fresk and G. Nikolakopoulos, "Full Quaternion Based Attitude Control for a Quadrotor," in *2013 European Control Conference*, 2013, pp. 3864–3869.
- [20] M. Fliess, J. Levine, P. Martin, and P. Rouchon, "Flatness and defect of non-linear systems: Introductory theory and examples," *International Journal of Control*, vol. 61, no. 6, pp. 1327–1361, 1995.
- [21] J. B. Kuipers, "Quaternion Algebra," in *Quaternions and Rotation Sequences*, 1999, pp. 103–139.
- [22] E. A. Coutsias and L. Romero, "The Quaternions with an application to Rigid Body Dynamics," Tech. Rep., 2004.
- [23] L. E. Beaver, M. Dorothy, C. Kroninger, and A. A. Malikopoulos, "Energy-Optimal Motion Planning for Agents: Barycentric Motion and Collision Avoidance Constraints," in *2021 American Control Conference (to appear)*, 2021.
- [24] L. E. Beaver and A. A. Malikopoulos, "An Energy-Optimal Framework for Assignment and Trajectory Generation in Teams of Autonomous Agents," *Systems & Control Letters*, vol. 138, 4 2020.